Customizable 3D braided composites made using a radial braiding machine based on the chain and sprocket design

C. Grandisson Arsenault[1], and L. Laberge Lebel[1*]

[1] Advanced Composites and Fibers Structures Laboratory (ACFSlab), High Performance Polymer and Composite Systems (CREPEC), Polytechnique Montreal, Montreal, Canada,

* *Corresponding author (LLL@polymtl.ca)*

Keywords: *3D braiding, textile composite, automated, chain and sprocket*

1. Abstract

Current products made from composite braids can rarely take advantage of their full mechanical potential because of the limitations of traditional two-dimensional and fixed geometry braiders. Assi et al. proposed a 3D hexagonal braider relying on the so-called chain and sprocket mechanism. The horngears (HG), i.e., the sprockets, were installed on a flat horizontal bedplate arranged in a hexagonal compact layout. The carrier had a chain shape that was moved by the HG. Since all HGs were individually controlled by independent motors, this design allowed the individual control of the tape carrier paths to achieve tailorable and evolutive braided structures. We present here a redesign of the chain and sprocket 3D braider in a radial configuration with an improve one-link chain carrier design. The objective was to demonstrate the customization ability of the 3D braider by manufacturing a braided tube with an evolving textile structure. The radial braiding machine structure was formed by a 48-sided polygon. It had seven axial layers of HGs, with 24 HGs on each circumferential layer, for a total of 168 HGs. The center of each HG was a tube to allow the passage of an axial tape. The full-scale braider was built. A Human-Machine-Interaction software was developed to program the rotations of HGs. To demonstrate the flexibility of the machine, continuous tubular textile was produced having a regular braid, followed by a diamond braid, and followed by a 2-layer filament winding. This braid was done using colored gift-wrapping tape on a 25.4 mm mandrel. To demonstrate the ability to braid several layers in one pass, 2-layer tubular braid, each layer having a diamond braid structure, was produced in one pass. The braid had a braiding angle of ± 60 °. The braided tapes were made using 24k carbon fiber tapes spread to a 5 mm width and preimpregnated with epoxy resin. The braid was done on a 25.4 mm diameter mandrel made of polyetherimide. The braid was oven-consolidated using heat shrink tape at 130 °C for 30 min, with heat-up and cooldown rates of 3 °C/min. The manufacturing of these prototypes paves the way for the braiding of complex preforms to be used in sports, automotive, and aerospace applications.

2. Introduction

Braids are used in structural composites for marine propellers, aircraft fuselage frame, and engines for their fatigue resistance and their crush properties [1-5]. The braiding process consists of intertwining yarns, unwinding from moving spools, to create a continuous structure [6]. Typical maypole braiding machines produce single layer two-dimensional (2D) braids. They use horngears (HGs) to move spool carriers along machined tracks. The braid architecture is mostly driven by the machine architecture. Different braid architectures require machine modifications. A tridimensional (3D) braid is a multilayered textile, where yarns of the braid connect every layer to each other. Therefore, 3D braids have yarns in the thickness's direction of the textile product, while 2D braids do not. 3D braid is less prone to delamination than a 2D braid, while a 2D braid has better mechanical properties in the braid axis compared to a 3D braid [5, 7].

The speed and the path taken by the carriers dictate the architecture of a braid. With the traditional braiders, the path followed by the carrier is fixed by the track and cannot be altered. The track limits the braided product to a fixed overall shape and architecture. To cope with the increasing forms and mechanical properties requirements, such for an intake manifold or turbine blades, a new braiding technology, allowing a complete control over the position and the carriers' path, is needed. Such technology could enable the fabrication of complex preforms with a continuous variable cross-section.

Several machine architectures were created to manufacture 3D braids. Bock et al. presented a mechanism similar to a railway switch, which is placed between HGs along the track, to modify the carrier path [8]. The switch can be activated to transfer the spool carriers between layers. Mungalov and Bogdanovich [9] designed the "rotary gripping fork" transfer mechanism, allowing to interchange two carriers between braided layers. A recent radial braider implemented an electromagnetic transfer mechanism for the same function [10]. Most braiding machines with a variable carrier path have a stepwise process. The machine must come to a complete stop when the carriers' path is altered. Additionally, each development still uses HGs that can house more than one carrier. When a HG rotates, every carrier's position located on it is altered. Hence, the displacement of the carrier cannot be totally controlled individually and independently. Another limitation of the technologies listed above is that some kind of switching device must be used in conjunction with the HGs. This adds up a layer of complexity in the machine architecture and control that limits the capability of braiding truly evolving fibrous structures.

Assi et al. developed a braider implementing a different carrier moving mechanism [11]. The "chain and sprocket" braider rely on a set of sprocket-shaped HGs, placed in a hexagonal packing arrangement on the same plane. The carrier has a chain shape with two links and three axes. The chain is always secured between two or three sprocket HGs. The carrier is moved by the rotation of the sprocket HGs in contact with the carrier chain. This simple design allows independent carrier movement essential for tailorable 3D braids, without the need for switching devices. The main limitation of the "chain and sprocket" braider is its size. Every circumferential layer of HGs added have six additional HGs compared to the previous layer. The quantity of independently controlled HGs soon becomes impractical for machines with more than seven layers.

This paper presents the redesign of the "chain & sprocket" braider in a radial configuration. The overview of the design is presented. Braid structures are made to demonstrate the machine functionality.

3. Overview of the chain & sprocket radial braider design

Figure 1a) shows an overview of the chain & sprocket radial braider design. The machine structure is 1.68 m wide by 1.68 m high, with a 1.2 m depth. There are 168 HGs sitting on hollow shafts.

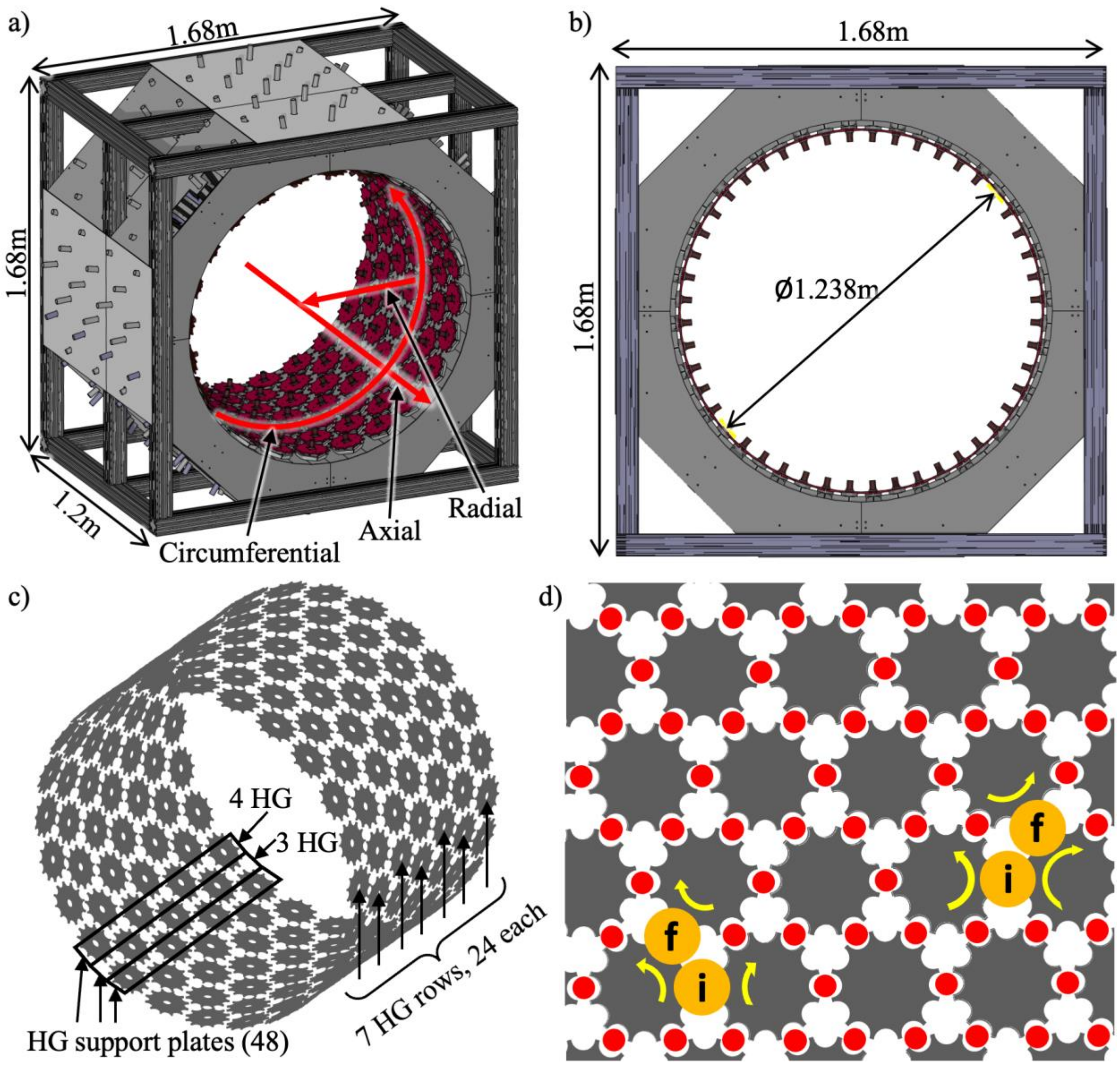

Figure 1. Chain & Sprocket radial braider overview. a) Overall dimensions and principal braider axes. b) Front view showing the 48 HG planes around the braider and braider diameter. c) 168 HGs arranged in a hexagonal packing on the circumferential-axial plane. There are seven rows of 24 HGs. The HGs are rotating around shafts connected to 48 HG support plates with three of four shafts each. d) View of the HG hexagonal packing on the circumferential-axial plane. The red dots are rest positions between two HGs, AKA nodes. There are two carrier movements from initial (i) to final (f) nodes with HG rotation directions.

The shafts are hollow to allow the passage of axial tapes through them. The shafts are connected to tubes going to the outside of the mechanical enclosure. The mechanical enclosure contains 168 stepper motors; each mounted with a drive. The motors precisely control the angular position of each HG through a 3:1 gearbox. The stepper motors are connected to a CAN-Open bus that communicates the target angular position. The braider axes system shown in Figure 1a) describes the circumferential-axial plane on which the HGs are distributed. The carriers, onto which tape unwinders are installed, are not shown on the Figure 1a). However, they are moved on this circumferential-axial plane with the rotations of the HGs (more details below). The braided tapes are pulled from the tape unwinders along the radial direction, to intertwine and form the braid in the center of the braider. This radial pulling of the tapes is typical of radial braiders. Figure 1b) shows front view of the braider with the circular arrangement of HGs. The diameter between the HG surfaces is 1.238 m. Figure 1c) shows the arrangement of HGs. The 168 HGs are divided in seven rows of 24 HGs. The HGs are placed in a hexagonal compact arrangement, according to Assi *et al.* design [11]. There are 48 HG support plates, with their normals pointing to the center of the braider. The HG support plates' normals are oriented with a $360°/48 = 7.5°$ angle between them. Twenty-four HG support plates have three HGs, and an altering 24 plates have four HGs. Figure 1d) schematize the carrier basic movements. It shows the hexagonal compact arrangement of HGs on the circumferential-axial plane. The HGs have a sprocket shape with 12 teeth and 12 notches. The red dots are rest positions between two HGs, that are identified as nodes. At every braiding step sequence, the carriers move between sequential nodes. The bottom-left yellow points indicate a carrier at an initial node i, that moves to its final node f to the top left. The right-hand-side yellow points indicate a carrier movement to the top-right. The arrows indicate the HG rotation directions needed to achieve these two carrier movements.

Figure 2 shows the mechanical components linking the HG movements to tape intertwining to create a braid. Figure 2a) shows a tape unwinder, mounted in a carrier being secured by two HGs. There are also the six brown hollow HG axes, with two of them showing an axial tape passing through. These tapes are pulled and intertwined between the braiding tapes, reinforcing the braid at an angle of 0° with respect to the axial direction. The HGs are mounted onto hubs that rotates around the HG hollow shafts. There are six shafts visible on Figure 2a), and two shafts hidden behind the tape unwinder. The shafts are connected to the HG support plates. There are 48 HG support plates placed at an angle of $180° - (360°/48) = 172.5°$ to cover the circumference of the braider. The HG support plates also secure the rails. The rails are injection molded with nylon. The carrier is composed of the slider and the chain. The slider is held by the rails and slides onto them. This interaction constrains the carrier onto the braider's circumferential-axial plane, so the carrier cannot fall due to the tape tension. Figure 2b-c) shows the side and front view of the slider. The grove on the side view (Figure 2b) is straight to guide the slider on the straight parts of the rails. The front and back of the carrier are open to help the carrier to embark on rails when moving from a node to another. Figure 2d) shows a top view of the carrier chain. The chain is composed of two axles linked together. The chain fits within the HG notches. It can be pushed by the rotation of the HGs. In summary, the carrier slider serves to maintain the carrier on the circumferential-axial plane, as well as to locate the carrier between HGs. The carrier chain serves to interact with the HGs to be pushed along a given carrier path.

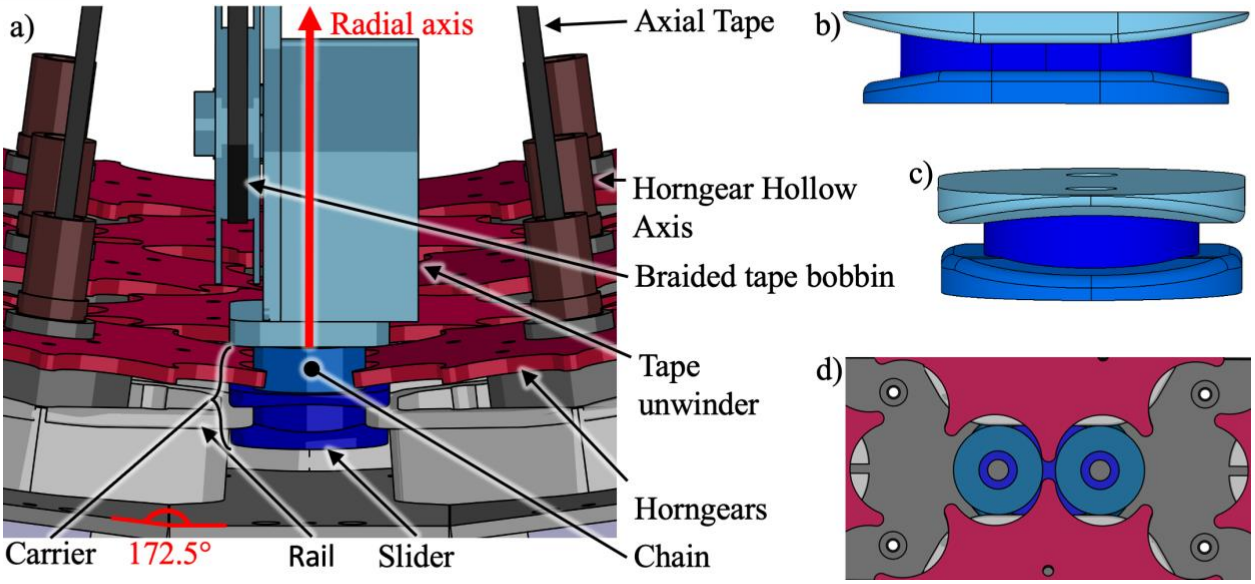

Figure 2. Mechanical components linking the HG to the tape. a) The HGs are parallel to the HG support plates. The HGs interact with the carrier chain. The carrier slider slides onto the rails below the HGs. The tape unwinder has a bobbin oriented to provide tape along the radial direction. Tapes can also pass through the hollow HG axes. b-c) side and front view of the slider with narrow side groves for guided movements on rails straight regions and open ends to facilitate the embarking on rails curved regions. d) Top view of the carrier chain with two axes located within the HG notches.

Figure 2a) also shows a tape unwinder. The tape unwinder has a tape bobbin with a rotation axis mostly tangent to the circumferential-axial plane. The unwinding rotation delivers the tape to the braid without unwanted twisting. The tape unwinder applies a constant tension during unwinding and can rewind the tape when there is slack in the tape.

Figure 3 shows the HG movement sequence to guide a carrier from one node to top right one. Figure 3a-e) shows the carrier chain interacting with HGs during the sequence. Figure 3 f-j) shows the interaction of the carrier slider with the rails. At Figure 3a) the carrier is initially located at a node between two HGs. Top and bottom HGs rotates by 30° to push the carrier to the right.

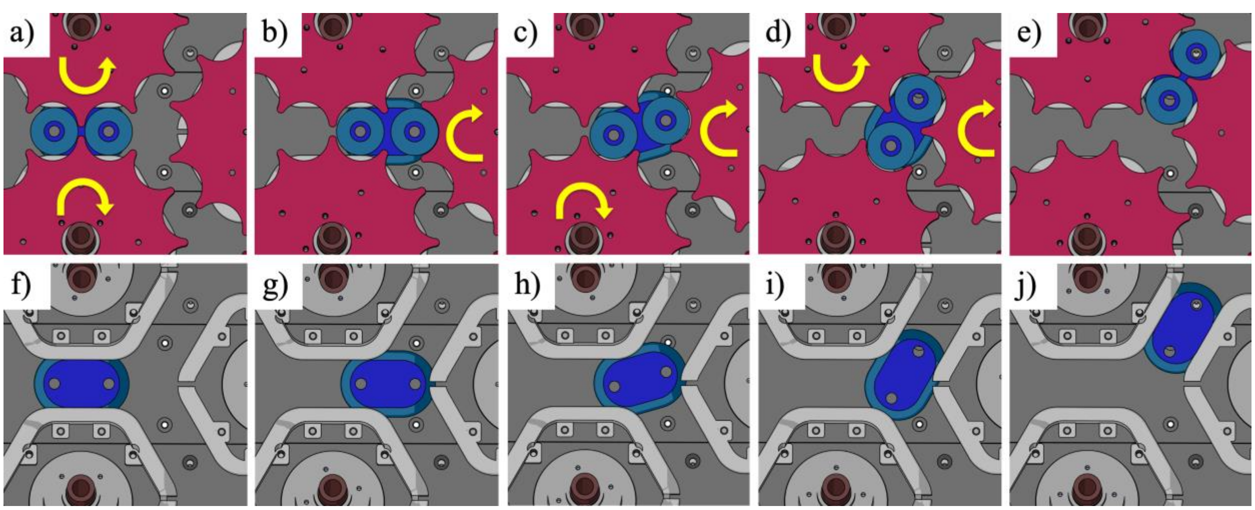

Figure 3. Carrier movement from a node to another. The sequence is divided in four steps from a) to d), resulting in e). a-e) Interaction between the HGs and the carrier chain. f-j) interaction between the slider and the rails.

The Figure 3f) shows that the rails between HGs are parallel, therefore, the carrier slider is moved in a straight direction towards the right-hand side (RHS) HG. At Figure 3b) the carrier is engaged in the RHS HG. Below the chain, the Figure 3g) shows that, at this position, the slider nose has engaged with the rails under the RHS HG. This HG will rotate by 6° along the clockwise direction to move the carrier nose to the top, as shown in Figure 3c). In Figure 3c) the bottom HG rotates clockwise by 15° and the RHS HG rotates clockwise by 9°. Figure 3g-i) show that during the carrier rotation, it is supported by the rails below the three HGs involved in the movement. These combined rotations result in orienting the carrier with the top right rails, as show in Figure 3i). The final segment of the sequence is a rotation from the top and RHS HGs to move the carrier at the node between the top and RHS HGs. During this final segment, the slider is constrained by the straight parts of the rails under the top and RHS HGs. Rotations can be assigned in the mostly similar sequence with reversed rotation directions. These HG rotation sequences are assigned to a dictionary of movements for all possible scenarios of carrier movements between nodes. The carrier paths are programmed using a human-machine interface (HMI) where the user can specify the incremental position of the carries on the nodes of the braider. Then the HMI translates the assigned position of carriers into HG rotation sequences.

4. Experimental

The first braid was made using colored gift-wrapping tape onto a 1-inch diameter polymer tube. Three textile structures were done without interruption. The Figure 4 shows the three carrier paths for the three textiles structures. Only half of the complete crown of the braider is shown, with 12 HG of the 24 HG per row in dark gray. Only three rows on the seven are shown. The yellow carriers moving to the right are the counterclockwise rotating carriers. The bleu carriers moving to the left are clockwise rotating carriers. There are six carriers, three on each direction, shown on the total of 12 carriers. Figure 4a) shows the regular braid structure. The paths of the carriers result in a pattern where every braided tape will pass over two braided tapes oriented along the other direction before passing below the next two, repetitively. This pattern is also called 2 over 2. The Figure 4b) shows the diamond braid structure. This pattern, also called 1 over 1, have every braided tape on one direction passing over only one braided tape before passing under the next one. The Figure 4c) shows a filament winding situation where six tapes are wrapped counterclockwise on the first layer, and overlaid with six tapes wrapped clockwise. For the first braid, the three sequences were programmed in a continuous fashion, one after the other. Two complete rotations of carriers were made for each sequence. The mandrel was hand-pulled to achieve a braiding angle close to 60°. The second braid was made with 24 carriers, 12 assigned to a first layer and 12 assigned to a second layer. The diamond braid (Figure 4b) was programmed for both layers. The first layer was started before for 4 complete rotations and then the second layer was started for 6 complete rotations. The mandrel was a Polyetherimide (PEI) rod of 1-inch diameter covered with a nylon bagging tube. The braided tapes were 24k carbon fiber tows pre-impregnated with low tack, b-staged epoxy resin (EzCiclo TPG3105-24H Towpreg, Swancore, S-Wanlai Co. Ltd.). The tapes had a nominal width of 5 mm. The overbraided mandrel was covered with release film (Wrightlon 3900, Airtech) and two layers of 1-inch-wide heat-shrink tape (6820A13, McMaster-Carr). The braid was oven-consolidated at 130 °C for 30 min, with heat-up and cooldown rates of 3 °C/min. After cooldown, the braid was removed from the mandrel to obtain a braided tube.

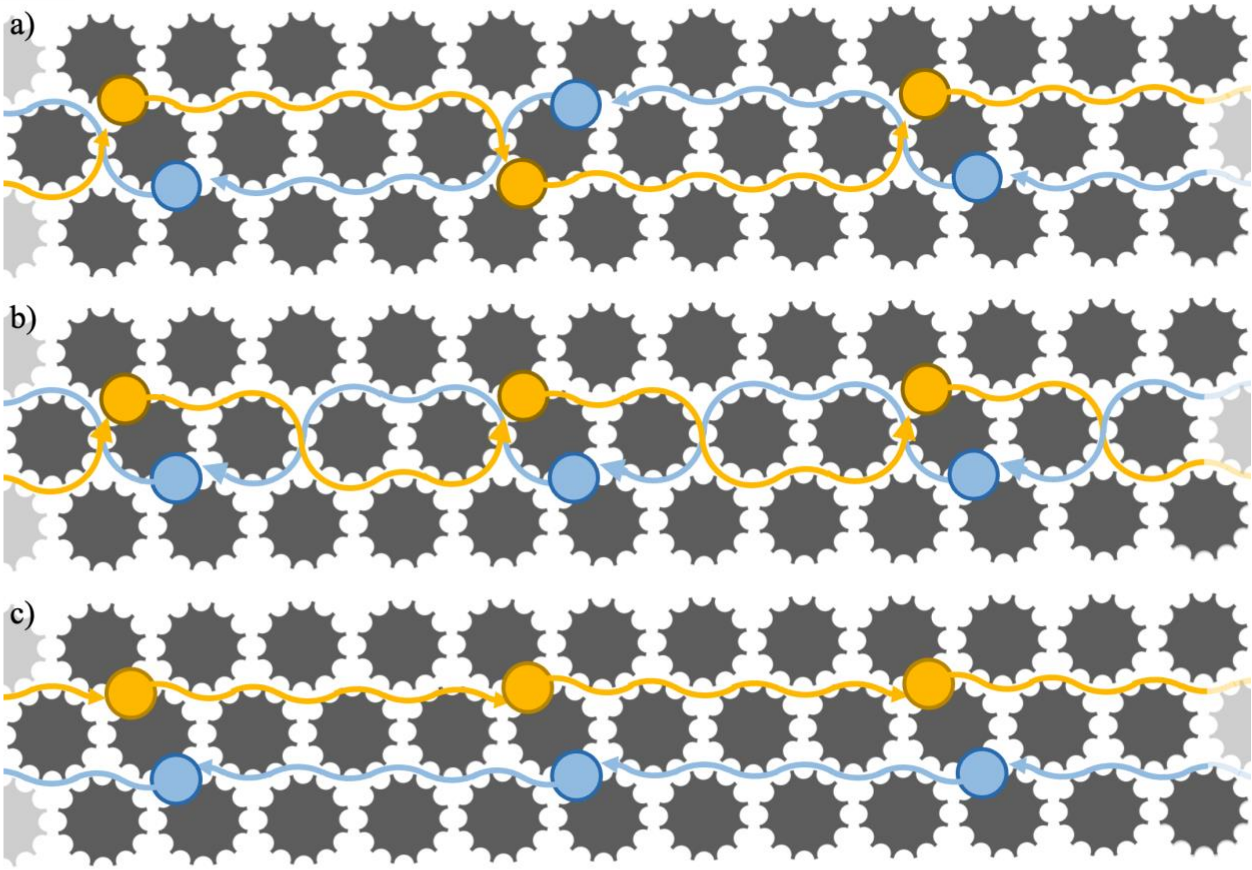

Figure 4. Carrier paths for three textile structures. Half of the complete braider crown is shown with three yellow carriers moving counterclockwise (six total) and three blue carriers moving clockwise (six total). Total number of braided tapes is 12. a) Regular braid structure (2 over 2). b) diamond braid structure (1 over 1). c) filament winding.

5. Results and Discussion

Figure 6 shows the braiding and obtained braided structures. Figure 6a) shows the gift-wrapping tape braiding with 12 tape unwinders spread on the braider crown. The tapes are exiting the carriers without twist towards the braid formation point onto the mandrel. Figure 6c) shows the obtain braid structure. Three distinct braid structures are seen: (i) the regular braid, (ii) the diamond braid, and (iii) the filament winding. Since there are two yellow tapes running counterclockwise, it can be seen on the regular and diamond braid parts that there are four yellow crossovers along the mandrel direction. It confirms that two complete rotations were made before changing the textile structure. Figure 6b) shows the braiding of the two-layer composite tube. It is seen that 24 carriers are feeding carbon fiber pre-impregnated tape towards the braided mandrel. The tapes are untwisted. Two distinct fell points are seen on the mandrel since the 12 carriers at the back of the braider lay-down the first braided layer, and the 12 carriers at the front of the braider lay-down the second braided layer. Since the first layer was started before, there is a distance between the braid fell points of the first and second layer. This allows the feeding tape angle with the mandrel to be similar. These similar braiding conditions result in similar braid angles between the first and second layer. Figure 6d) shows a top view of the consolidated braided composite tube. The small, curved lines along the tube are most probably resin-rich lines created with the resin flow into the release film wrinkles. The tapes appear mostly flat showing that the braiding process did not provoke unwanted twist of the tapes. The two braids shown in Figure 6 demonstrate the braiding machine ability to braid changing textiles structures in one pass, and multiple layers in one pass. The braided structures shown in Figure 6c,d) were made in around eight minutes. This speed is rather low compared to typical radial braiders. The slow braiding process is mainly attributed with the HG rotations pausing between rotation steps of each simple carrier movement sequence. Future work will improve the movement sequence to reduce the number of steps and therefore reducing the pause events.

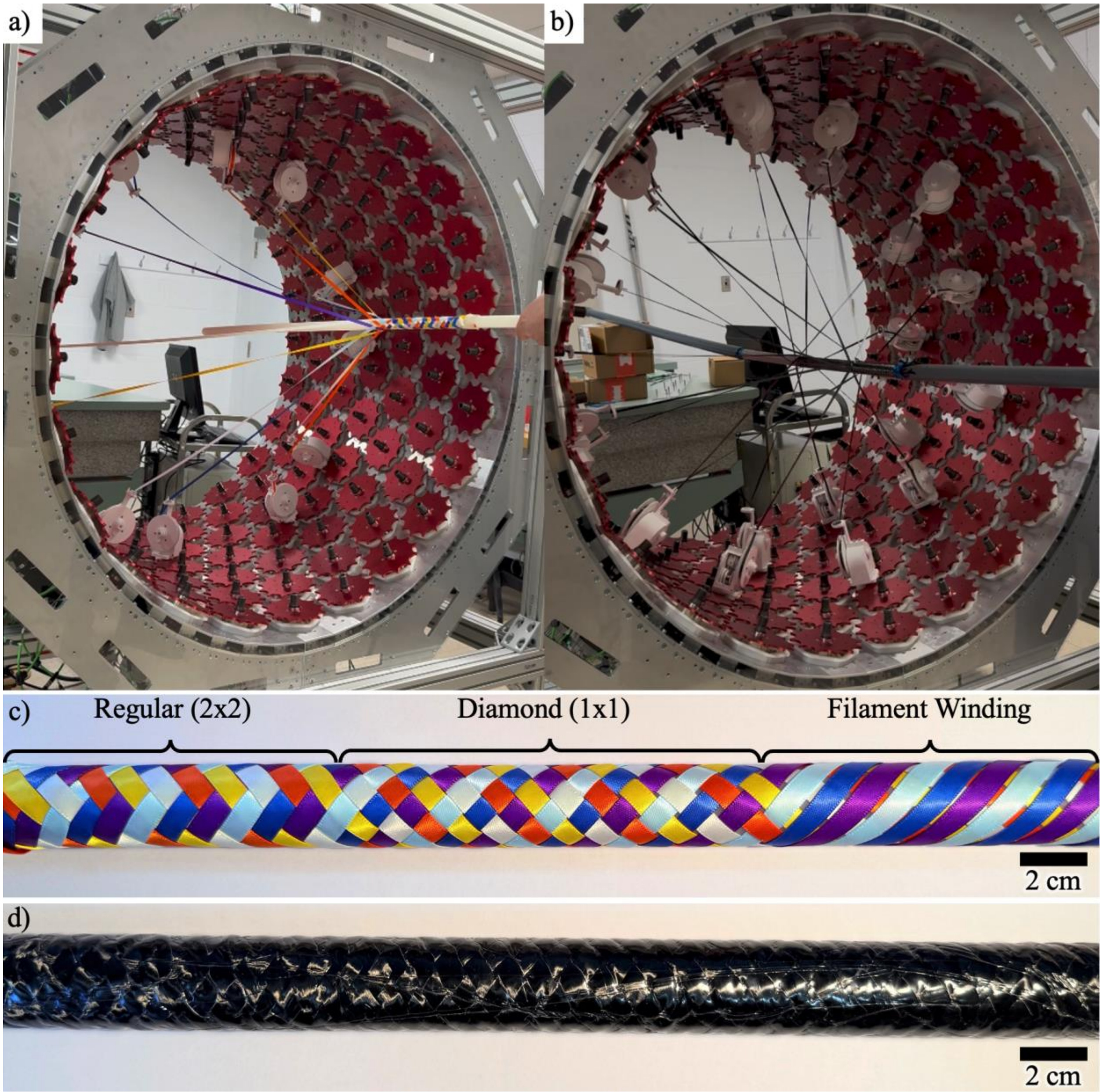

Figure 6. Braiding demonstrations. a),c) single layer braid with 12 gift-wrapping tape showing a regular, a diamond and a filament winding structure for two rotations each. b),d) two-layer braided tube made with carbon prepreg tapes. The PEI mandrel is secured by thick polymer tubes.

6. Conclusion

This study introduces a chain-and-sprocket braider in a radial arrangement. The braider has seven circumferential rows of 24 HG arranged in a hexagonal compact packing. The carriers are composed of a chain part that is pushed by sprocket-like HG, and a slider part that orient the carrier movements. The carriers are equipped with tape unwinders. The two braided structures demonstrate the flexibility of this machine. A regular braid, followed by a diamond braid, and followed by a filament winding was made without interruptions. This structure is unachievable by conventional braiders. The second structure was a 2-layer composite braided tube made in one pass. This second structure demonstrates the higher material lay down rates achievable, as well as the possibility to manufacture carbon/epoxy structures. The development of the radial chain-and-sprocket 3D braider paves the way for the braiding of complex preforms to be used in sports, automotive, and aerospace applications.

7. Acknowledgements

This project was funded by the NSERC I2IPJ 598148 – 24 grant.

8. References

[1] H. Hamada. “Can braided composites be used for crushing elements in cars? ”. *Proceedings of ICCM-11, Gold Coast, Australia, 1997*
[2] M. Okano, A. Nakai, and H. Hamada. "Axial crushing performance of braided composite tubes". *International Journal of Crashworthiness*, Vol. 10, No. 3, pp. 287-94, 2005.
[3] P. Potluri, A. Rawal, M. Rivaldi, and I. Porat. "*Geometrical modelling and control of a triaxial braiding machine for producing 3D preforms". ICMAC 2001*. pp. 481-92, 2003.
[4] Y. Qiang, S. Zhihong, Q. Yiping, Z. Shenhua, C. Yanting, W. Jiewei, *et al*. "Study on the braiding of preform with special-shaped sections based on the two-dimensional braiding process". *Textile Research Journal*, Vol. 89, No. 2, pp. 172-81, 2019.
[5] W. Zhipeng, Z. Guoli, Z. Youxin, Z. Liqing, S. Xiaoping, and W. Weiwei. "Theoretical analysis of braiding strand trajectories and simulation of three-dimensional parametric geometrical models for multilayer interlock three-dimensional tubular braided preforms". *Textile Research Journal*, Vol. 89, No. 19-20, pp. 4306-22, 2019.
[6] Y. Kyosev. "Advances in Braiding Technology: Specialized Techniques and Applications", 2016,
[7] K. Bilisik. "Three-dimensional braiding for composites: A review". *Textile Research Journal*, Vol. 83, No. 13, pp. 1414-1436, 2013.
[8] K. Bock and G. Flohr, "Process and machine for production of braided packing", Patent no. US4096781A. USPTO, 1975.
[9] D. Mungalov and A. Bogdanovich, "Automated 3-D braiding machine and method", Patent no. US6439096B1, USPTO, 2001.
[10] H.F. Potzsch, M. Brauner, K. Lehmann, F. Budillon, C. Cherif, and D. Aibibu. "3D rotary tunnel braiding system with active control: algorithm and structure formation for complex braided designs", 2026. https://doi.org/10.1007/s00170-026-17696-4
[11] P. Assi, S. Achiche, and L. Laberge Lebel. "3D printing process for textile composites". *CIRP Journal of Manufacturing Science and Technology*, Vol. 32, No., pp. 507-16, 2021.